International Dairy Journal 88 (2019) 25–33

Contents lists available at ScienceDirect

International Dairy Journal

journal homepage: www.elsevier.com/locate/idairyj

Interaction between calcium and casein hydrolysates: Stoichiometry, binding constant, binding sites and thermal stability of casein phosphopeptide complexes

Ricardo Troncoso Recio [a, *], Nelson P. Guerra [a], Ana Torrado [a], Leif H. Skibsted [b]

[a] Department of Analytical and Food Chemistry, Faculty of Science, Ourense Campus, University of Vigo, Ourense, Spain
[b] Department of Food Science, University of Copenhagen, Rolighedsvej 30, DK-1958, Frederiksberg C, Denmark

ARTICLE INFO

Article history:
Received 18 June 2018
Received in revised form
15 August 2018
Accepted 15 August 2018
Available online 27 August 2018

ABSTRACT

The ability of a casein hydrolysate rich in casein phosphopeptides (CPPs) to form calcium complexes was studied. An association constant of 125 ± 32 L mol^{-1} at 25 °C was determined electrochemically, forming 1:1 complexes according to conductivity measurements. Chloride anions increased the affinity for calcium and number of CPPs bound to calcium in solution to more than one. From temperature dependence of the association constant, the enthalpy of binding of calcium chloride to CPPs was determined to be −24 kJ mol^{-1}. Fourier transform infrared spectroscopy confirmed solid state binding of chloride and calcium to CPPs, further showing a positive cooperativity induced by calcium due to opening of the alpha-helix structure of CPPs. In addition, calcium chloride complexation was shown to increase the thermal stability of CPPs according to the results of thermogravimetry differential scanning calorimetry. In conclusion, hydrolysed casein could be considered as a potential enhancer of calcium availability in food.

1. Introduction

Casein phosphopeptides (CPPs) are phosphorylated peptides from hydrolysis of casein, the main protein of milk, which is distributed through α_{S1}-, α_{S2}-, β- and κ-casein fractions in the ratio 3:0.8:3:1 (Park & Allen, 1998). CPPs, like the native protein, are reported to exhibit calcium binding properties, which is primarily attributed to the negatively charged region of their primary structure, consisting of three phosphoserines followed by two glutamic acids, also called the 'acidic motif' (Ferraretto, Gravaghi, Fiorilli, & Tettamanti, 2003). The calcium chelation of CPPs prevents calcium interaction with anions (e.g., phosphates, oxalates, phytates or palmitates) from food during digestion in the neutral to alkaline conditions of intestine, which otherwise leads to precipitation. Therefore, calcium solubility under these conditions is promoted by the presence of CPPs (FitzGerald, 1998; Skibsted, 2016; Sun et al., 2016). This makes this compound interesting from a nutritional point of view, since the combination of CPPs with calcium might be the basis of novel calcium fortified foods and food supplements with high calcium availability.

Much research has been conducted to characterise the Ca-CPP interaction using purified CPP products (Berrocal et al., 1989; Ellegård, Gammelgård-Larsen, Sørensen, & Fedosov, 1999; Meisel & Olieman, 1998; Mekmene & Gaucheron, 2011; Zong, Peng, Zhang, Lin, & Feng, 2012). However, from the most practical perspectives of the food industry, the study of the interaction between calcium and casein hydrolysates (CHs) (containing CPPs) seems to be interesting so as to determine the calcium binding capacity of the whole CH product instead of CPPs specifically, since CHs are more accessible than purified CPPs for the food industry. In fact, the interaction of calcium and protein hydrolysates has previously been studied in calcium fortified food based on milk proteins (Canabady-Rochelle, Sanchez, Mellema, & Banon, 2009a) or soy protein hydrolysates (Canabady-Rochelle, Sanchez, Mellema, & Banon, 2009b). A high calcium binding capacity was observed in these studies, suggesting such proteins as promising carriers for calcium fortification of food. However, casein hydrolysate interaction with calcium clearly needs further study.

For characterisation of the Ca–CH interaction, it seems necessary to determine the stoichiometry of the species involved in the complex formed. It will also be useful for the determination of the

* Corresponding author. Tel.: +34 678 056 437.
E-mail address: ricardo.troncoso@uvigo.es (R.T. Recio).

https://doi.org/10.1016/j.idairyj.2018.08.009
0958-6946/

binding constant of the complex, since it depends on the number of ligands involved in calcium chelation. For this purpose, the method of Continuous Variations, also known as Job's method, is a simple and commonly used procedure (Hill & MacCarthy, 1986; Renny, Tomasevich, Tallmadge, & Collum, 2013; Rossotti & Rossotti, 1961). This method is based on the measurement of any physical property, such as absorbance or conductivity (Renny et al., 2013), that correlates linearly with the concentration of the formed metal-ligand complex (M-L_n).

Therefore, the aim of this work was to characterise the interaction between calcium and a casein hydrolysate product (containing 24% CPP). For this purpose, the stoichiometry of the calcium and CH complex was determined by the Job's method conductivity-based, the calcium binding constant of the CH was determined electrochemically and the temperature dependence was studied applying van't Hoff equation. Additionally, the calcium and CH complex was structurally characterised by Fourier transform infrared (FT-IR) spectroscopy, and the thermal stability of the complex was studied by thermogravimetry-differential scanning calorimetry (TG-DSC).

2. Materials and methods

2.1. Chemicals

$CaCl_2.2H_2O$ and $Ca(CF_3SO_3)_2$ [calcium triflate; $Ca(OTf)_2$] were obtained from Merck (Darmstadt, Germany) and Sigma–Aldrich (Steinheim, Germany), respectively. The commercial product Hyvital Casein Phosphopeptides, purchased from FrieslandCampina Domo (Amersfoort, The Netherlands) was used as a source of casein hydrolysates. This product consists of casein hydrolysates at a 17% degree of hydrolysis with an average molecular mass of 600 Da, of which 24% are casein phosphopeptides (CPPs). The product contains 91.3% protein, 5.0% moisture and 6.2% ash.

2.2. Job's method or method of Continuous Variations

Table 1 presents the samples prepared for the Job's method, which consisted of solutions made at 7 different $CaCl_2$ and CH concentrations keeping fixed the total solution concentration at 0.020 mol L^{-1} to obtain 7 different points. Additionally, samples with only one component at each point were prepared. All solutions were prepared using purified water from Milli-Q Plus (Millipore Corporation, Bedford, MA, USA), and stirring the samples for 1 h at 25 °C before conductivity measurements. The experiment was repeated by using $Ca(OTf)_2$ as a source of calcium, instead of $CaCl_2$.

Table 1
Job's method design.[a]

Point	X_{Ca}	*Ca* (mol L^{-1})	*CH* (mol L^{-1})	C_{total} (mol L^{-1})
1	0.00	0.0000	0.0200	0.0200
	0.00	0.0000	0.0167	0.0167
2	0.17	0.0033	0.0167	0.0200
	0.17	0.0033	0.0000	0.0033
	0.00	0.0000	0.0133	0.0133
3	0.33	0.0067	0.0133	0.0200
	0.33	0.0067	0.0000	0.0067
	0.00	0.0000	0.0100	0.0100
4	0.50	0.0100	0.0100	0.0200
	0.50	0.0100	0.0000	0.0100
	0.00	0.0000	0.0067	0.0067
5	0.67	0.0133	0.0067	0.0200
	0.67	0.0133	0.0000	0.0133
	0.00	0.0000	0.0033	0.0033
6	0.83	0.0167	0.0033	0.0200
	0.83	0.0167	0.0000	0.0167
7	1.00	0.0200	0.0000	0.0200

[a] Abbreviations are: X_{Ca}, calcium mole fraction; *Ca*, calcium concentration; *CH*, casein hydrolysate concentration; C_{total}, total concentration of the solution. Duplicate experiments were performed using $CaCl_2.2H_2O$ or $Ca(OTf)_2$ as sources of calcium.

When the molar fraction of $CaCl_2$ (X_M) approaches 0, all the metal is considered to be complexed. On the other hand, when the molar fraction of the calcium salt approaches 1, all the ligand is presumed to be in the complexed form. Considering that conductivity is mainly due to the uncomplexed species, the theoretical point of minimum conductivity calculated by extrapolation, as shown in Fig. 1, is considered the stoichiometric ratio between the metal and the ligand for complex formation. The number of ligands, *n*, is obtained by the ligand/metal ratio of the complex in the point of minimum conductivity according to equation (1):

$$n = \frac{C_L^{min}}{C_M^{min}} = \frac{(1 - X_M)}{X_M} \quad (1)$$

The Job's method used in this work was based on conductivity (κ) according to the linear relationship found with the concentration of reagents (Supplementary material Fig. S2). Following the procedure described by Stapelfeldt, Jun, and Skibsted (1993), the conductivity of the complex was calculated as the difference between the conductivity of the reacting samples and the conductivity if no reaction had occurred (samples with only one component at the same concentration as the combined sample) following the equation (2):

$$\kappa_{complex} = \kappa_{combined\ sample} - \kappa_{Ca(non-reacting)} - \kappa_{CH(non-reacting)} \quad (2)$$

2.3. Conductivity measurement

The conductivity measurements for the Job's method were carried out at 25 °C by a 4-pole conductivity cell, model CDC866T (Radiometer, Copenhagen, Denmark), calibrated with a 0.01D KCl standard solution (1408 μS cm^{-1}). Each measurement was obtained after stirring for 1 min to stabilise the measurement (Garcia, Vavrusova, & Skibsted, 2016).

2.4. Sample preparation for binding constant determination

Samples for binding constant determination were solutions prepared at a constant $CaCl_2$ concentration (1×10^{-3} mol L^{-1}) and increasing CH concentrations (1×10^{-3}, 2×10^{-3}, 5×10^{-3}, 1×10^{-2}, 2×10^{-2}, 3×10^{-2} and 5×10^{-2} mol L^{-1}). The same CH concentrations were used in the case of $Ca(OTf)_2$, which was used at a concentration of 1×10^{-3} mol L^{-1}. All solutions were prepared using purified water from Milli-Q Plus (Millipore Corporation).

2.5. Electrochemical measurement of calcium ion activity

For the calcium ion activity determination, samples were stirred for 1 h at 25 °C in a climate chamber before the analysis and the measurement by a selective electrode ISE25Ca with a reference REF251 electrode from Radiometer was performed at 25 °C using a water bath with temperature control, following the procedure described by Vavrusova and Skibsted (2016). For the temperature dependence experiment, the same procedure was used but calibrated and measured at 25, 30, 35, 40 and 45 °C using the corresponding Debye-Hückel constant (0.510, 0.515, 0.520, 0.525, and 0.530, respectively) for the calculation of the activity coefficient by the Davies' equation. Based on calcium ion activity, free calcium concentration was calculated by using the same methodology.

2.6. Temperature dependence of the binding constant

Solutions of 1×10^{-3} mol L^{-1} CH and 1×10^{-2} mol L^{-1} $CaCl_2$ were prepared and stirred for 1 h at 25, 35 and 40 °C before measuring the potential to calculate the K_c at each temperature as previously described. All solutions were prepared using purified water from Milli-Q Plus (Millipore Corporation). The application of van't Hoff equation (3) to the different K_c obtained at different temperatures allowed the calculation of the thermodynamic parameters ΔH° and ΔS°:

$$lnK_c = -\frac{\Delta H^\circ}{RT} + \frac{\Delta S^\circ}{R} \quad (3)$$

2.7. Sample preparation for Fourier transform infrared spectroscopy and thermogravimetry differential scanning calorimetry

Five samples for FT-IR and TG-DSC were prepared initially in aqueous solution: 0.01 mol L^{-1} CH control (CH); 0.1 mol L^{-1} $CaCl_2$ control ($CaCl_2$); 0.001 mol L^{-1} Ca and 0.01 mol L^{-1} CH (1Ca–CH); 0.01 mol L^{-1} Ca and 0.01 mol L^{-1} CH (2Ca–CH); and 0.1 mol L^{-1} Ca and 0.01 mol L^{-1} CH (3Ca–CH). Samples were stirred at 25 °C for 1 h to ensure the complete reaction and subsequently frozen at −80 °C for 2 days. The water was then removed by lyophilisation in a LyoQuest freeze dryer (Telstar, Catalunya, Spain) at −85 °C and 0.01 mbar for 3 days.

2.8. Fourier transform infrared spectroscopy

Infrared spectra were recorded at room temperature in two different ranges using a Nicolet 6700 FT-IR spectrophotometer (Thermo scientific, Waltham, MA, USA) operating in transmission mode. In the case of medium IR range (400–4000 cm^{-1}), about 1 mg of dried lyophilised sample was mixed with 100 mg of KBr. The mixtures were homogenised using a mortar and pestle, and then pressed at 6 Ton forming a pellet that was placed in a sample holder. Each sample was scanned 32 times at a wavenumber resolution of 4 cm^{-1} using a deuterated triglycine sulphate (DTGS) detector and a KBr beamsplitter. For far IR (200–600 cm^{-1}) measurements, pressed pellets of lyophilised samples mixed with CsI were required. In this case, a solid substrate beamsplitter and DTGS polyethylene detector were used.

Deconvolution of amide I peak (1600–1700 cm^{-1}) was applied to analyse the secondary structure of casein hydrolysate samples. For this purpose, a Gaussian curve fitting analysis with a linear baseline and various FWHH (full width at half height) were performed with OMNIC software to find the best fit. This analysis was carried out by the CACTI Ourense support service of the University of Vigo. The interpretation of secondary structures from deconvoluted spectra was performed dividing the fractional area of each peak by the sum of the areas of the peaks that comprise the amide I band, following the procedure of Litvinov, Faizullin, Zuev, and Weisel (2012). The assignment of the peaks to specific secondary structures was based on previous works (Boye, Ma, & Harwalkar, 1997; Byler & Farrell, 1989; Litvinov et al., 2012).

2.9. Thermogravimetry – differential scanning calorimetry

Lyophilised samples of CH, $CaCl_2$ and mixtures of both compounds, contained in hermetic pans, were analysed in a TG-DSC Setsys Evolution 16/18 thermal analyser (Setaram, Caluire, France) to assess the changes in mass and energy produced by the increasing temperature in the range of 25–250 °C at a heating rate of 5 °C min^{-1}. An empty pan was used as a reference. This analysis was carried out by the CACTI Ourense support service of the University of Vigo.

3. Results and discussion

3.1. Stoichiometry; Job's method

For determination of the stoichiometry of the complex between calcium and CH, the Job's method was applied for the reactions of CH with calcium triflate ($Ca(OTf)_2$) and calcium chloride ($CaCl_2$), and the Job plots obtained are shown in Fig. 1A,B, respectively. The Job plot obtained with $Ca(OTf)_2$ showed a minimum conductivity at 0.42 calcium mole fraction (X_{Ca}) for the extrapolated points (Fig. 1A), indicating that calcium is chelated by only 1 ligand molecule (CH) or, in other words, 1:1 Ca:CH stoichiometry, to form the Ca–CH complex. However, in the case of $CaCl_2$, the minimum conductivity was obtained at 0.35 X_{Ca} for the extrapolated points (Fig. 1B), indicating that calcium would be chelated by 2 ligand (CH) molecules, giving a 1:2 Ca:CH stoichiometry. Considering that the triflate counter-anion is inert (Taube & Scott, 1971), only calcium and CH can be involved in the reaction with $Ca(OTf)_2$. Therefore, a 1:1 Ca:CH stoichiometry was stablished for the Ca–CH complex and accordingly, 1:1 Ca:CH was used for the calculation of the binding constant. The fact that 1:2 Ca:CH ratio was obtained in the case of $CaCl_2$ suggests that chloride played a role in the complex formation. It is likely that the negatively charged chloride species (Cl^-) have interacted with the positively charged domains of CH structure (such as arginine, histidine and lysine residues or forming hydrogen bridges with hydrogen from hydroxyl groups). This interaction seems to increase the number of CH molecules (probably CPPs) able to react with calcium, obtaining a stoichiometry higher than 1:1. The CH-chloride interaction was further analysed in the FT-IR section (Fig. 6).

3.2. Binding constant

As in the previous section, the calcium and CH reaction was studied in two series of experiments, between $Ca(OTf)_2$ and CH, and between $CaCl_2$ and CH, and the measurement of the potential of these solutions allowed the binding constants to be determined, considering 1:1 stoichiometry in both $CaCl_2$ and $Ca(OTf)_2$ cases according to the Job plot for the complex of interest (Ca–CH) (Fig. 1A). The binding constants obtained are shown in Tables 2 and 3.

For the reaction between $Ca(OTf)_2$ and CH, the binding constant presented an average value of 125 ± 32 L mol^{-1}, ranging from 68 ± 4 and 158 ± 10 L mol^{-1} (Table 2). Considering that CH is a casein hydrolysate product containing 24% CPP, these results are consistent with the range of binding constants (from 38 to 599 L mol^{-1}) reported for CPP by other researchers (Berrocal et al., 1989; Ellegård et al., 1999; Mekmene & Gaucheron, 2011; Park & Allen, 1998; Park, Swaisgood, & Allen, 1998; Zong et al., 2012). These observations indicate a calcium binding affinity of CH comparable to that of purified CPP products. In the case of CH reacting with $CaCl_2$, the binding constant showed an average value of 298 ± 101 L mol^{-1} ranging from 142 ± 1 and 436 ± 35 L mol^{-1} (Table 3). These values were higher than those obtained in the case of $Ca(OTf)_2$, suggesting that the interaction of chloride with the positively charged regions of the hydrolysate leads to an increase in the CH affinity for calcium.

Furthermore, the value of the binding constant showed a decrease with increasing CH concentrations (Tables 2 and 3), which was unexpected since a change in concentrations should not affect the binding constant. The change in the binding constant with

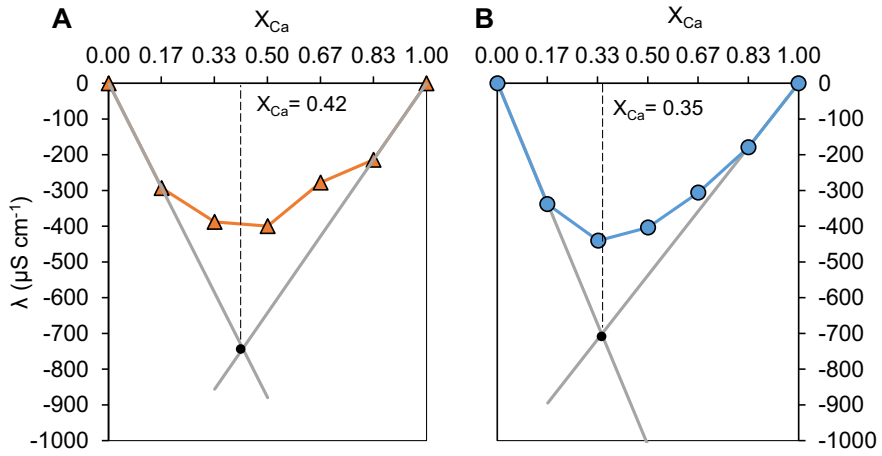

Fig. 1. (A) Job plots of the reactions between $Ca(OTf)_2$ and CH (triangles) in water showing a minimum at 0.42 calcium mole fraction for extrapolated points, and (B) between $CaCl_2$ and CH (circles) showing a minimum at 0.35 calcium mole fraction for the extrapolated points.

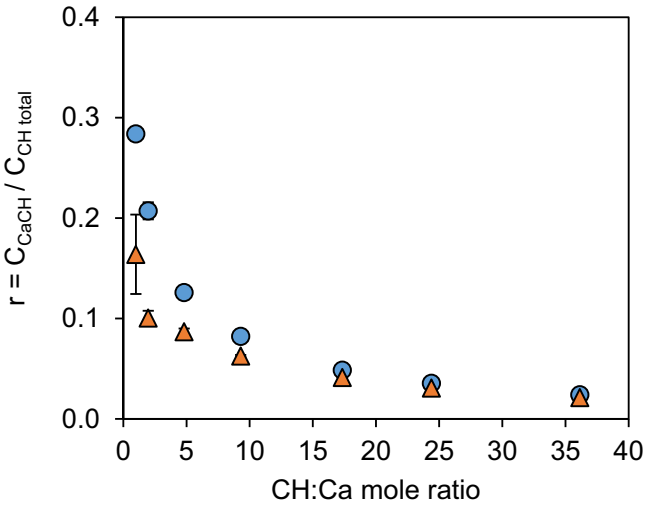

Fig. 2. Specific binding capacity (r) of CH with two sources of calcium: $CaCl_2$ 0.001 mol L^{-1} (circles) and $Ca(OTf)_2$ 0.001 mol L^{-1} (triangles) with increasing CH concentrations.

different CH concentrations was also reflected in the specific binding capacity (r) of CH, since r also decreased with increasing CH concentrations (Fig. 2).

The lower the CH concentration (left side of Fig. 2), which is equivalent to higher Ca:CH ratio, the higher the ability of CH to form complex. This suggests that a change in the structure of CH or a rearrangement in the charges of CH takes place when calcium binds CH, which increases calcium affinity or accessibility for the

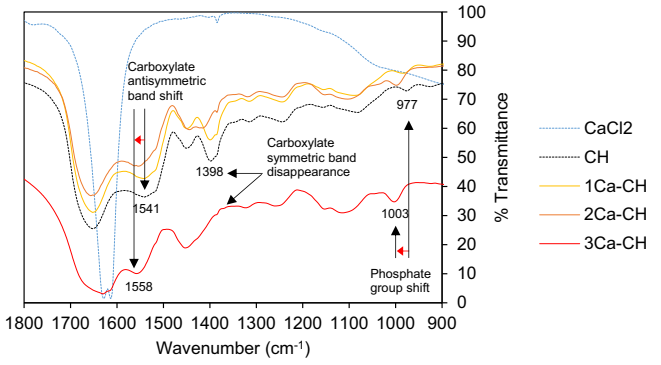

Fig. 4. FT-IR spectra (900–1800 cm^{-1} region) of $CaCl_2$, CH, 1Ca–CH, 2Ca–CH and 3Ca–CH solid samples.

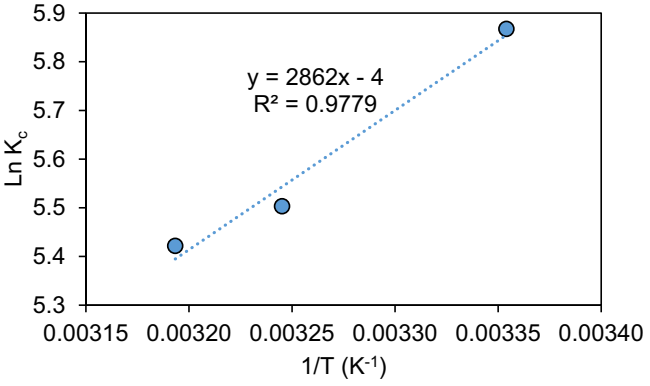

Fig. 3. van't Hoff plot showing the effect of temperature on the binding constant for the $CaCl_2$ and CH reaction in water.

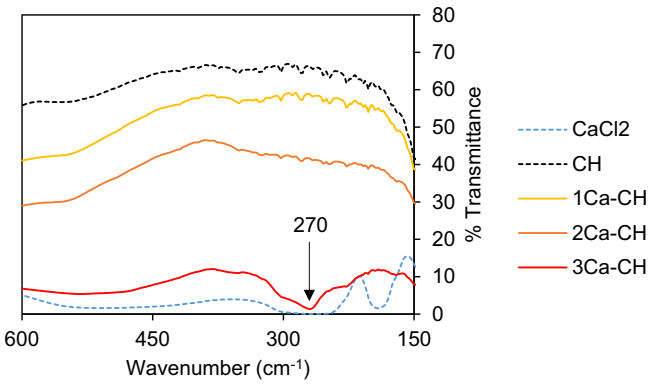

Fig. 5. Far FT-IR spectra (150–600 cm^{-1}) of $CaCl_2$, CH, 1Ca–CH, 2Ca–CH and 3Ca–CH solid samples.

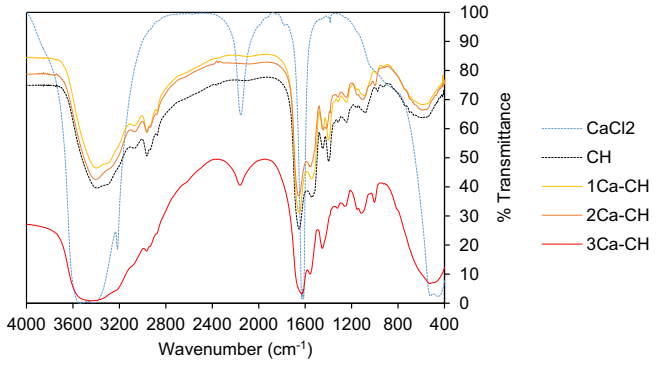

Fig. 6. Medium FT-IR spectra (400–4000 cm^{-1}) of $CaCl_2$, CH, 1Ca–CH, 2Ca–CH, and 3Ca–CH solid samples.

other binding sites. CH binds higher amounts of calcium in the equilibrium under these conditions, as it was reported for the interaction between calcium and a lipopeptide, which produced a change in structure that enhanced the accessibility of other binding sites (Nasir et al., 2013).

The calcium induced structural change is in agreement with the findings of Cross, Huq, Bicknell, and Reynolds (2001), who reported a change in structure of β-CPPs upon calcium addition. This phenomenon might be characterised as positive cooperativity induced by calcium as it was observed for the "EF-hand" motif contained in proteins, such as calmodulin, troponin or calcineurin (Busch, Hohenester, Timpl, Paulsson, & Maurer, 2000; Gifford, Walsh, & Vogel, 2007; Maune, Klee, & Beckingham, 1992). This change in the specific binding capacity with different CH concentrations was observed for both $CaCl_2$ and $Ca(OTf)_2$ (Fig. 2), and it was also noticed that the specific binding capacity obtained for the $Ca(OTf)_2$ system was significantly lower ($P < 0.05$) than that of $CaCl_2$ at low CH concentrations (left side of Fig. 2). These observations are in agreement with the lower binding constants obtained for $Ca(OTf)_2$ compared with $CaCl_2$, suggesting again that chloride might play an important role in the calcium and CH association reaction. Fig. 2 also shows that at CH:Ca ratios higher than 17, both systems showed a similar behaviour, indicating that a great CH excess does not affect positively the binding capacity of CH for both calcium salts.

3.3. Temperature dependence of the binding constant

Temperature dependence of the binding constant was analysed using the binding constant determined at 25, 35 and 40 °C, and applying van't Hoff equation (3) for the case of $CaCl_2$ and CH with the concentrations of 0.001 and 0.01 mol L^{-1}, respectively. Assuming the 1:1 stoichiometry also in the case of $CaCl_2$ and CH, the relationship between the $\ln(K_c)$ with the inverse of temperature was found to be linear, with a high R^2 value of 0.98 (see Fig. 3).

From the van't Hoff plot for the binding constant (Fig. 3), the binding heat (ΔH°) and the change in entropy (ΔS°) for calcium to CH binding in presence of chloride were determined to be −23.8 kJ mol^{-1} (indicating exothermic reaction for the formation of the complex) and −31.1 J mol^{-1} K^{-1}, respectively. The negative values of both ΔH° and ΔS° suggests that the driving forces of the calcium and CH association process are van der Waals interactions and hydrogen bonding, according to Ross and Subramanian (1981) and Zhang, Geng, Haung, and Ma (2016).

3.4. Fourier transform infrared spectroscopy

3.4.1. Binding sites

Differences in IR spectra of solid state samples of casein hydrolysates in the absence and presence of calcium indicate calcium-CH interaction and may point at specific binding sites of CH involved in calcium coordination. Fig. 4 shows the IR spectra in the range of 900–1800 cm^{-1} of CH alone, $CaCl_2$ alone and CH with increasing calcium concentrations (1Ca–CH, 2Ca–CH and 3Ca–CH) in solid state. The far IR spectra (150–600 cm^{-1}) and the complete IR medium spectra (400–4000 cm^{-1}) are shown in Figs. 5 and 6, respectively.

Focussing on the 900–1800 cm^{-1} region, the band at 977 cm^{-1} of CH control (Fig. 4), assigned to phosphate group (Kumar et al., 2015), was shifted to 999 and 1003 cm^{-1} in the two samples with the highest calcium content (2Ca–CH and 3Ca–CH). This indicates

Table 2
Binding constant, K_c, pH values and ionic strength (I) for the reaction between $Ca(OTf)_2$ and different concentrations of casein hydrolysate (CH) in water at 25 °C.[a]

$Ca(OTf)_2$ (mol L^{-1})	Ca (mol L^{-1})	CH (mol L^{-1})	CH:Ca mole ratio	pH	I (mol L^{-1})	K_c (L mol^{-1})
0.001	1.02×10^{-3}	0.002	2	6.9	3.6×10^{-3}	137 ± 13
0.001	1.04×10^{-3}	0.005	5	7.0	4.8×10^{-3}	158 ± 10
0.001	1.08×10^{-3}	0.010	9	7.0	7.0×10^{-3}	148 ± 6
0.001	1.15×10^{-3}	0.020	17	7.1	1.2×10^{-2}	132 ± 5
0.001	1.23×10^{-3}	0.030	24	7.1	1.7×10^{-2}	104 ± 0
0.001	1.38×10^{-3}	0.050	36	7.1	2.7×10^{-2}	68 ± 4
0.001	1.00×10^{-3}	0.000	–	5.8	3.0×10^{-3}	–
0.000	3.84×10^{-4}	0.050	130	7.1	2.6×10^{-2}	–

[a] Ca concentration corrected with Ca from CH.

Table 3
Binding constant (K_c), pH values and ionic strength (I) for the reaction between $CaCl_2$ and different concentrations of casein hydrolysate (CH) in water and at 25 °C.[a]

$CaCl_2$ (mol L^{-1})	Ca (mol L^{-1})	CH (mol L^{-1})	CH:Ca mole ratio	pH	I (mol L^{-1})	K_c (L mol^{-1})
0.001	1.02×10^{-3}	0.002	2	6.9	3.2×10^{-3}	436 ± 35
0.001	1.04×10^{-3}	0.005	5	7.0	4.4×10^{-3}	352 ± 3
0.001	1.08×10^{-3}	0.010	9	7.0	6.6×10^{-3}	353 ± 1
0.001	1.15×10^{-3}	0.020	17	7.1	1.1×10^{-2}	281 ± 7
0.001	1.23×10^{-3}	0.030	24	7.1	1.7×10^{-2}	224 ± 0
0.001	1.38×10^{-3}	0.050	36	7.1	2.7×10^{-2}	142 ± 1
0.001	1.00×10^{-3}	0.000	–	6.0	3.0×10^{-3}	–
0.000	3.84×10^{-4}	0.050	130	7.1	2.5×10^{-2}	–

[a] Ca concentration corrected with Ca from CH.

that the phosphate group of CH plays an important role in calcium coordination, as expected due to the calcium binding ability of phosphorylated serine residues (Berrocal et al., 1989; Mekmene & Gaucheron, 2011; Phelan, Aherne, Fitzgerald, & O'Brien, 2009).

The bands at 1398 and 1541 cm^{-1} of the CH spectrum (Fig. 4) were assigned to the COO^- symmetric (υ_s) and antisymmetric (υ_{as}) stretches in agreement with Byler and Farrell (1989) and Nara, Morii, and Tanokura (2013). These are two vibration modes of the O–C–O bonds, which are present in the carboxylate groups of aspartate and glutamate residues. The vibration mode is symmetric (υ_s) when the stretching vibrations of both C–O bonds are in phase and antisymmetric (υ_{as}), when C–O stretching vibrations are out-of-phase with another (Byler & Farrell, 1989). The addition of calcium produced changes in COO^- υ_s and υ_{as} bands, being more pronounced in the sample containing the highest calcium content (3Ca–CH). The symmetric band at 1398 cm^{-1} of CH disappeared in the presence of calcium (3Ca–CH, Fig. 4) as occurred in the case of casein, in which, the symmetric band at 1400 cm^{-1} became a weak shoulder after calcium addition, as reported by Byler and Farrell (1989). On the other hand, the antisymmetric band shifted from 1541 cm^{-1} in CH control to 1558 cm^{-1} in the 3Ca–CH sample (Fig. 4). According to Nara et al. (2013), this band is characteristic of calcium coordination by a carboxylate group (reported for 1553 cm^{-1}). These two changes in the C–O vibration bands in presence of calcium suggest that the carboxylate groups from side chain of aspartate and glutamate residues of CH are also involved in calcium bonding, which is in agreement with the findings of Byler and Farrell (1989) for casein, also in solid state.

Another significant difference between CH and 3Ca–CH spectra was observed in the far IR region (Fig. 5). While the CH control sample showed a quite regular spectrum without noticeable bands, 3Ca–CH showed a band at 270 cm^{-1}, that might be assigned to the Ca–O vibration mode, since according to Lu, Deng, Miao, and Li (2003), the Ca–O bond will be found in the far IR region 200 to 400 cm^{-1}.

3.4.2. Effect of chloride

A clear effect of the chloride counterion was noted in the broad band in the 3200–3500 cm^{-1} region (Fig. 6) associated to the O–H and N–H bonds (Ren et al., 2015), which reflects the hydrogen-bond network formed between hydroxyl groups and water molecules (Lu et al., 2003). Comparing CH and 3Ca–CH (which contains $CaCl_2$) spectra in this region, a wider band was observed in case of the sample with calcium chloride (3Ca–CH). This may be the result of a rearrangement of the hydrogen–bonding network produced by chloride forming O–H···Cl···H–O interactions reinforcing the structure, as it was reported by Lu et al. (2003) for the complex formed between calcium chloride and D-ribose. Indeed, these researchers pointed out that the chloride–OH interactions were not only intramolecular but also intermolecular, suggesting that in this case, chloride might be interacting with two molecules of CH, playing an important role. Notably, this is in agreement with the results of Job's method, which indicated a 1:2 Ca:CH stoichiometry for the case of $CaCl_2$ and CH (Fig. 1B).

3.4.3. Secondary structure

The amide I band region (1600–1700 cm^{-1}) has been widely studied to determine the type of secondary structure of proteins (Boye et al., 1997; Byler & Farrell, 1989; Byler & Susi, 1986; Litvinov et al., 2012; O'Loughlin, Kelly, Murray, FitzGerald, & Brodkorb, 2015). Amide I band represents the vibration of the peptide backbone bonds, mainly the C=O stretching vibration and, to a lesser extent, the out-of-phase C–N stretching vibration, the C–C–N deformation and the N–H in-plane bend (Barth, 2007). Amide I band can accordingly indicate the different secondary structure elements of a protein and subsequently, structural changes produced by the presence of calcium can be detected monitoring the amide I band in the IR spectrum. To separate the components involved in the amide I band, the original IR spectrum was deconvoluted and the narrow bands obtained were quantified and assigned to a secondary structure element following the procedure of Litvinov et al. (2012).

Fig. 7 shows the amide I band deconvolution of CH, 1Ca–CH, 2Ca–CH and 3Ca–CH solid samples and Supplementary material Tables S1–S8 show the peaks and areas obtained in each case. The assignment of each peak to a secondary structure was based on the following: the α-helix structures are mainly detected at 1654 cm^{-1}, random coil is detected at 1645 cm^{-1} and β-structures

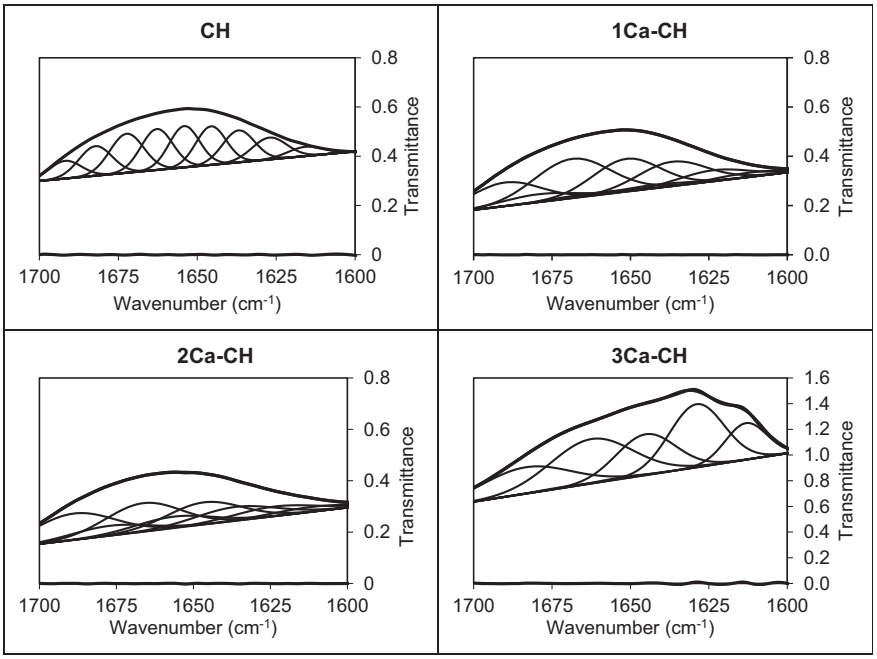

Fig. 7. Amide I band deconvolution in the 1600–1700 cm^{-1} region of CH, 1Ca–CH, 2Ca–CH and 3Ca–CH solid samples.

are detected at 1692 cm^{-1} and below 1635 cm^{-1} according to Byler and Farrell (1989) and Boye et al. (1997). In addition, turns are reflected at 1664 and 1676 cm^{-1} according to Litvinov et al. (2012). After the assignment of each peak to a secondary structure, the area of each peak (corresponding to one specific secondary structure) was divided by the sum of the areas of the peaks that comprise the amide I band, giving the percentage of each secondary structure in the sample, and the results are shown in Table 4.

Solid samples with increasing calcium concentrations obtained different peak areas, indicating a change in secondary structure of casein hydrolysates dependent on calcium concentration, similarly to the changes produced in a lipopeptide structure upon calcium addition, which were dependent on calcium concentration (Nasir et al., 2013).

The solid CH without calcium presented a 14% α-helix, which was almost completely lost in the higher calcium content sample (3Ca–CH), which only presented a 0.5% α-helix (Table 4). Contrary, β-structures, turns, loops and random coils increased in the sample with the higher calcium content (Table 4). This suggests that the initial helix became part of β-sheets, turns, loops and random coils upon calcium addition. These results are in agreement with those reported by Byler and Farrell (1989), according to which, the % α-helix of casein decreased when calcium was added to casein. The same researchers further suggested that some calcium binding sites (amino acid residues) of casein, initially hidden in the helix structure, might have become more accessible after the interaction of calcium due to the induced partial uncoil, enhancing the affinity for calcium. The results of Cross et al. (2001) also support the change in the secondary structure reported in the present work, since they observed a change in β-CPP(1–25) structure towards turns and loops upon calcium addition using nuclear magnetic resonance (NMR) spectroscopy. The reduction in α-helix structure upon calcium addition suggested in the present work was also observed for fibrin clots upon compression, being the deformation produced through the coiled-coils, and in the case of bovine serum albumin under stress and other filamentous proteins like α-keratin, desmin and vimentin (Litvinov et al., 2012).

Table 4
Secondary structures of solid samples of casein hydrolysates without calcium (CH) and with increasing calcium concentrations (1Ca–CH, 2Ca–CH, and 3Ca–CH), obtained by the deconvolution of amide I band.

Type of secondary structure	CH	1Ca–CH	2Ca–CH	3Ca–CH
α-helix (%)	14	21	8.8	0.5
β-structures (%)	31	42	45	37
turns/loops/random coils (%)	55	38	46	63

3.5. Thermal stability

The effect of Ca complexation on the above-mentioned changes of the secondary structure of the peptides in solid state were investigated studying the thermal stability of solid samples with increasing calcium concentration, 1Ca–CH, 2Ca–CH, and 3Ca–CH, and solid control samples CH and $CaCl_2$, through TG-DSC between 25 and 250 °C. The DSC and TG thermograms are shown in Fig. 8A,B, respectively.

In this analysis two main thermal patterns were observed (Fig. 8A). The sample in which $CaCl_2$ is the majority species (3Ca–CH) presented a similar profile to that of the pure salt ($CaCl_2$), showing a major thermal event at around 150 °C (Fig. 8A), while 1Ca–CH and 2Ca–CH samples presented a profile closer to that of the CH pure species, characterised by a peak at 84 °C, which is probably due to dehydration, and other two endothermic peaks at 164 and 196 °C (Fig. 8A), both ascribed to denaturation events involving the secondary structure of the peptides. These two denaturation peaks were gradually lost with increasing calcium chloride concentrations, since 1Ca–CH conserved both peaks, 2Ca–CH did not show the first peak and 3Ca–CH lost both (Fig. 8A). The disappearance of the first denaturation peak in 2Ca–CH sample suggests that the secondary structure denatured at 164–166 °C in CH and 1Ca–CH was not present in 2Ca–CH. According to FT-IR results, the 2Ca–CH contained lower α-helix than CH and 1Ca–CH (Table 4), so the endothermic peak at 164–166 °C in CH and 1Ca–CH could accordingly be attributed to the partial unfolding of α-helix in agreement with the suggestion of Ren et al. (2015), who reported α-helix denaturation at 149 °C for casein hydrolysates. In addition, the higher denaturation temperature observed for the second denaturation peak in the case of 2Ca–CH (210 ± 1 °C) with respect to 1Ca–CH (200 ± 1 °C) and CH (196 ± 2 °C) suggests that calcium chloride enhanced the thermal stability of CH. This is probably related to the structural change towards more β-structures and random coils induced by calcium chloride, according to FT-IR results (Table 4). This stabilising effect could also be due to the role of chloride species enhancing the complexing ability of CH, as described above also with regard to the FT-IR analysis. Indeed, no denaturation peaks were detected in the sample with higher calcium chloride content (3Ca–CH) in the

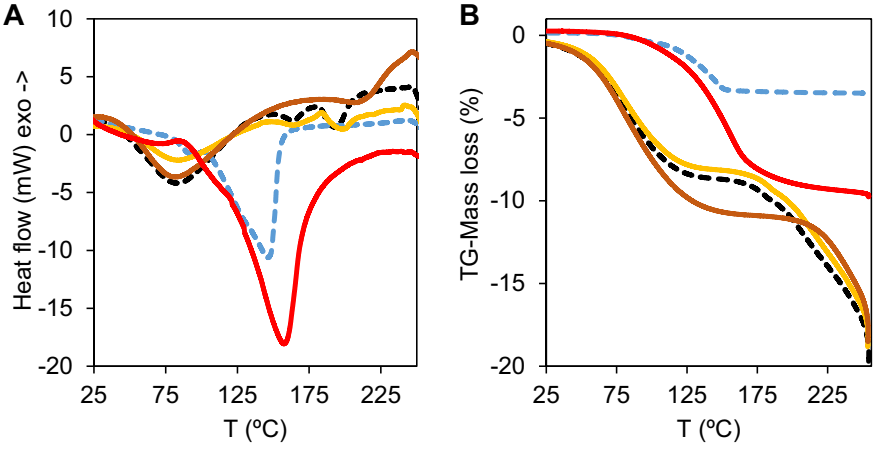

Fig. 8. (A) DSC and (B) TG thermograms of CH (black dashed line), $CaCl_2$ (blue dashed line), 1Ca–CH (yellow line), 2Ca–CH (brown line) and 3Ca–CH (red line) solid samples performed at 5 °C min^{-1} from 25 to 250 °C.

studied temperature range (25–250 °C), which might appear at higher temperatures in the same way as what happened with the displacement of the peak at 196 ± 2 °C of CH to 200 ± 1 and 210 ± 1 °C in 1Ca–CH and 2Ca–CH, respectively, or the peak around 147 ± 1 °C of $CaCl_2$ shifted to 158 ± 2 °C in 3Ca–CH.

Moreover, in agreement with the findings of Cai, Lin, and Wang (2017), Cai, Yang, Lin, Fu, and Wang (2017), and Zhao et al. (2014), the significant lower total mass loss in the case of 3Ca–CH (−10 ± 0%) with respect to CH without calcium (−2 0 ± 0%) after the full thermal treatment (see Fig. 8B at 250 °C) indicated better thermal stability for the complex than for the casein hydrolysate without calcium chloride.

4. Conclusions

The product of casein hydrolysates (CH) with 24% CPP studied in the present work has calcium binding ability comparable to other hydrolysed proteins according to the binding constant obtained. Carboxylate and phosphate groups of CH were suggested as the main calcium binding sites, based on FT-IR analyses. A higher specific binding capacity was observed for higher Ca:CH ratios. Deconvoluted FT-IR spectra indicated a change in structure from α-helix towards β-structure, turns and random coil upon calcium addition inducing positive cooperativity for calcium binding. The missing denaturation peak in the TG-DSC thermogram at 164–166 °C of solid state samples with higher calcium content confirmed such positive cooperativity induced by calcium. The higher binding constant obtained with $CaCl_2$ compared to $Ca(OTf)_2$ suggests that chloride anion promotes calcium binding capacity of CH. In addition, Cl^- seems to increase the number of CPPs associated to the complex by intermolecular hydrogen bonds with different molecules of CPP. The formation of a complex with calcium chloride increases the thermal stability of CH according to the results of TG-DSC.

Acknowledgements

The authors thank Drs Martina Vavrusova and André C. García (University of Copenhagen) for their valuable assistance with binding constant and conductivity methodologies, and Lisbet Snedstrup Christensen (University of Copenhagen) for providing language help. This study was supported by the University of Vigo [predoctoral research stay grant)].

Appendix A. Supplementary data

Supplementary data related to this article can be found at https://doi.org/10.1016/j.idairyj.2018.08.009.

References

Barth, A. (2007). Infrared spectroscopy of proteins. *Biochimica et Biophysica Acta (BBA) Bioenergetics, 1767*, 1073–1101.
Berrocal, R., Chanton, S., Juillerat, M. A., Favillare, B., Scherz, J.-C., & Jost, R. (1989). Tryptic phosphopeptides from whole casein. II. Physicochemical properties related to the solubilization of calcium. *Journal of Dairy Research, 56*, 335–341.
Boye, J. I., Ma, C.-I., & Harwalkar, V. R. (1997). Thermal denaturation and coagulation of proteins. In S. Damodaran, & A. Paraf (Eds.), *Food proteins and their applications* (pp. 25–56). New York, NY, USA: Marcel Dekker, Inc.
Busch, E., Hohenester, E., Timpl, R., Paulsson, M., & Maurer, P. (2000). Calcium affinity, cooperativity, and domain interactions of extracellular EF-hands present in BM-40. *Journal of Biological Chemistry, 275*, 25508–25515.
Byler, D. M., & Farrell, H. M., Jr. (1989). Infrared spectroscopic evidence for calcium Ion interaction with carboxylate groups of casein. *Journal of Dairy Science, 72*, 1719–1723.
Byler, D. M., & Susi, H. (1986). Examination of the secondary structure of proteins by deconvolved FTIR spectra. *Biopolymers, 25*, 469–487.
Cai, X., Lin, J., & Wang, S. (2017a). Novel peptide with specific calcium-binding capacity from *Schizochytrium* sp. protein hydrolysates and calcium bioavailability in Caco-2 cells. *Marine Drugs, 15*, 15010003.
Cai, X., Yang, Q., Lin, J., Fu, N., & Wang, S. (2017b). A specific peptide with calcium-binding capacity from defatted *Schizochytrium* sp. protein hydrolysates and the molecular properties. *Molecules, 22*, 22010544.
Canabady-Rochelle, L.-S., Sanchez, C., Mellema, M., & Banon, S. (2009a). Thermodynamic characterization of calcium-milk protein interaction by isothermal titration calorimetry. *Dairy Science & Technology, 89*, 257–267.
Canabady-Rochelle, L.-S., Sanchez, C., Mellema, M., & Banon, S. (2009b). Study of calcium - soy protein Interactions by isothermal titration calorimetry and pH cycle. *Journal of Agricultural and Food Chemistry, 57*, 5939–5947.
Cross, K. J., Huq, N. L., Bicknell, W., & Reynolds, E. C. (2001). Cation-dependent structural features of beta-casein-(1-25). *Biochemical Journal, 356*, 277–286.
Ellegård, K. H., Gammelgård-Larsen, C., Sørensen, E. S., & Fedosov, S. (1999). Process scale chromatographic isolation, characterization and identification of tryptic bioactive casein phosphopeptides. *International Dairy Journal, 9*, 639–652.
Ferraretto, A., Gravaghi, C., Fiorilli, A., & Tettamanti, G. (2003). Casein-derived bioactive phosphopeptides: Role of phosphorylation and primary structure in promoting calcium uptake by HT-29 tumor cells. *FEBS Letters, 551*, 92–98.
FitzGerald, R. J. (1998). Potential uses of caseinophosphopeptides. *International Dairy Journal, 8*, 451–457.
Garcia, A. C., Vavrusova, M., & Skibsted, L. H. (2016). Calcium d-saccharate: Aqueous solubility, complex formation, and stabilization of supersaturation. *Journal of Agricultural and Food Chemistry, 64*, 2352–2360.
Gifford, J., Walsh, M., & Vogel, H. (2007). Structures and metal-ion-binding properties of the Ca2+-binding helix-loop-helix EF-hand motifs. *Biochemical Journal, 405*, 199–221.
Hill, Z. D., & MacCarthy, P. (1986). Novel approach to Job's method: An undergraduate experiment. *Journal of Chemical Education, 63*, 162–170.
Kumar, B. S., Hemalatha, T., Deepachitra, R., Raghavan, R. N., Prabu, P., & Sastry, T. P. (2015). Biphasic calcium phosphate-casein bone graft fortified with *Cassia occidentalis* for bone tissue engineering and regeneration. *Bulletin of Materials Science, 38*, 259–266.
Litvinov, R. I., Faizullin, D. A., Zuev, Y. F., & Weisel, J. W. (2012). The α-helix to β-sheet transition in stretched and compressed hydrated fibrin clots. *Biophysical Journal, 103*, 1020–1027.
Lu, Y., Deng, G., Miao, F., & Li, Z. (2003). Sugar complexation with calcium ion. Crystal structure and FT-IR study of a hydrated calcium chloride complex of d-ribose. *Journal of Inorganic Biochemistry, 96*, 487–492.
Maune, J. F., Klee, C. B., & Beckingham, K. (1992). Ca2+ binding and conformational change in two series of point mutations to the individual Ca(2+)-binding sites of calmodulin. *Journal of Biological Chemistry, 267*, 5286–5295.
Meisel, H., & Olieman, C. (1998). Estimation of calcium-binding constants of casein phosphopeptides by capillary zone electrophoresis. *Analytica Chimica Acta, 372*, 291–297.
Mekmene, O., & Gaucheron, F. (2011). Determination of calcium-binding constants of caseins, phosphoserine, citrate and pyrophosphate: A modelling approach using free calcium measurement. *Food Chemistry, 127*, 676–682.
Nara, M., Morii, H., & Tanokura, M. (2013). Coordination to divalent cations by calcium-binding proteins studied by FTIR spectroscopy. *Biochimica et Biophysica Acta (BBA) Biomembranes, 1828*, 2319–2327.
Nasir, M. N., Laurent, P., Flore, C., Lins, L., Ongena, M., & Deleu, M. (2013). Analysis of calcium-induced effects on the conformation of fengycin. *Spectrochimica Acta Part A Molecular and Biomolecular Spectroscopy, 110*, 450–457.
O'Loughlin, I. B., Kelly, P. M., Murray, B. A., FitzGerald, R. J., & Brodkorb, A. (2015). Concentrated whey protein ingredients: A Fourier transformed infrared spectroscopy investigation of thermally induced denaturation. *International Journal of Dairy Technology, 68*, 349–356.
Park, O., & Allen, J. C. (1998). Preparation of phosphopeptides derived from αs-casein and β-casein using immobilized glutamic acid-specific endopeptidase and characterization of their calcium binding. *Journal of Dairy Science, 81*, 2858–2865.
Park, O., Swaisgood, H. E., & Allen, J. C. (1998). Calcium binding of phosphopeptides derived from hydrolysis of αs-casein or β-casein using immobilized trypsin. *Journal of Dairy Science, 81*, 2850–2857.
Phelan, M., Aherne, A., Fitzgerald, R. J., & O'Brien, N. M. (2009). Casein-derived bioactive peptides: Biological effects, industrial uses, safety aspects and regulatory status. *International Dairy Journal, 19*, 643–654.
Renny, J. S., Tomasevich, L. L., Tallmadge, E. H., & Collum, D. B. (2013). Method of Continuous Variations: Applications of Job plots to the study of molecular associations in organometallic chemistry. *Angewandte Chemie International Edition, 52*, 11998–12013.
Ren, X., Pan, D., Wu, Z., Zeng, X., Sun, Y., Cao, J., et al. (2015). Limited hydrolysis of β-casein by cell wall proteinase and its effect on hydrolysates conformational and structural properties. *International Journal of Food Science and Technology, 50*, 55–61.
Rossotti, F. J. C., & Rossotti, H. (1961). *The determination of stability constants and other equilibrium constants in solution*. New York, NY, USA: McGraw-Hill Book Company, Inc.
Ross, P. D., & Subramanian, S. (1981). Thermodynamics of protein association reactions: Forces contributing to stability. *Biochemistry, 20*, 3096–3102.
Skibsted, L. H. (2016). Mineral nutrient interaction: Improving bioavailability of calcium and iron. *Food Science and Biotechnology, 25*, 1233–1241.
Stapelfeldt, H., Jun, H., & Skibsted, L. H. (1993). Fluorescence properties of carminic acid in relation to aggregation, complex formation and oxygen activation in aqueous food models. *Food Chemistry, 48*, 1–11.

Sun, N., Wu, H., Du, M., Tang, Y., Liu, H., Fu, Y., et al. (2016). Food protein-derived calcium chelating peptides: A review. *Trends in Food Science & Technology, 58*, 140–148.

Taube, H., & Scott, A. (1971). Complexing tendency of trifluoromethylsulfonate ion as measured using chromium(III). *Inorganic Chemistry, 10*, 62–66.

Vavrusova, M., & Skibsted, L. H. (2016). Aqueous solubility of calcium citrate and interconversion between the tetrahydrate and the hexahydrate as a balance between endothermic dissolution and exothermic complex formation. *International Dairy Journal, 57*, 20–28.

Zhang, X., Geng, F., Huang, X., & Ma, M. (2016). Calcium binding characteristics and structural changes of phosvitin. *Journal of Inorganic Biochemistry, 159*, 76–81.

Zhao, L., Huang, Q., Huang, S., Lin, J., Wang, S., Huang, Y., et al. (2014). Novel peptide with a specific calcium-binding capacity from whey protein hydrolysate and the possible chelating mode. *Journal of Agricultural and Food Chemistry, 62*, 10274–10282.

Zong, H., Peng, L., Zhang, S., Lin, Y., & Feng, F. (2012). Effects of molecular structure on the calcium-binding properties of phosphopeptides. *European Food Research and Technology, 235*, 811–816.